ELSEVIER

Chemosphere 62 (2006) 731–740

CHEMOSPHERE

www.elsevier.com/locate/chemosphere

# Competitive adsorption of dye metanil yellow and RB15 in acid solutions on chemically cross-linked chitosan beads

Ming-Shen Chiou *, Guo-Syong Chuang

*Department of Chemical Engineering, National United University, Miao Li 360, Taiwan, ROC*

Received 13 July 2004; received in revised form 26 April 2005; accepted 27 April 2005
Available online 20 June 2005

**Abstract**

One kind of adsorbent with a high adsorption capacity for anionic dyes was prepared using ionically and chemically cross-linked chitosan beads. A batch system was applied to study the adsorption behavior of one acid dye (MY, metanil yellow) and one reactive dye (RB15, reactive blue 15) in aqueous solutions by the cross-linked chitosan beads. The adsorption capacities was 3.56 mmol $g^{-1}$ (1334 mg $g^{-1}$) for dye MY and 0.56 mmol $g^{-1}$ (722 mg $g^{-1}$) for dye RB15 at pH 4, 30 °C. The Langmuir model agreed very well with the experimental data ($R^2 > 0.996$). The kinetics of adsorption for a single dye and the kinetics of removal of ADMI color value in mixture solutions at different initial dye concentrations were evaluated by the nonlinear first-order and second-order models. The first-order kinetic model fits well with the dynamical adsorption behavior of a single dye for lower initial dye concentrations, while the second-order kinetic model fits well for higher initial dye concentrations. The competitive adsorption favored the dye RB15 in the mixture solution (initial conc. (mM): MY = 1.34; RB15 = 1.36); while it favored the dye MY in the mixture solution (initial conc. (mM): MY = 3.00; RB15 = 1.34) and the adsorption kinetics for dye RB15 has the tendency to shift to a slower first order model.


*Keywords:* Adsorption capacity; Anionic dyes; Cross-linked chitosan beads; Langmuir isotherm; Competitive adsorption

## 1. Introduction

Color effluents have been produced ever since the dyeing technique was invented. Various kinds of synthetic dyestuffs appear in the effluents of wastewater in various industries such as dyestuff, textiles, leather, paper, etc. Concern exits since a very small amount of dye in water is highly visible and may be toxic to aquatic creatures. Some toxic dyes, particularly benzidine or arylamine based dyes are well known for their carcinogenity (Choudhary, 1996; Yu et al., 2002). Hence, the removal of color synthetic organic dyestuff from waste effluents becomes environmentally important. It is rather difficult to treat dye effluents because of their synthetic origins and their mainly aromatic structure, which are biologically nondegradable. Among several chemical and physical methods, adsorption process is one of the effective techniques that have been successfully employed for color removal from wastewater. Many adsorbents have been tested to reduce dye concentrations from aqueous solutions. Activated carbon (Rao and Ashutosh, 1994; Allen, 1996) is regarded as an effective but expensive adsorbent due to its high costs of

* Corresponding author. Tel.: +886 37 381570; fax: +886 37 332397.
*E-mail address:* chiou@nuu.edu.tw (M.-S. Chiou).

0045-6535/$ - see front matter © 2005 Elsevier Ltd. All rights reserved.
doi:10.1016/j.chemosphere.2005.04.068

manufacturing and regeneration. Out of economic consideration, it is not used to treat a large quantity of effluents by a great scale of activated carbon. In addition to activated carbon, some adsorbents including peat (Ramakrishna and Viraraghavan, 1997), chitin (McKay et al., 1983), silica (McKay, 1984) and some agriculture wastes (Low and Lee, 1997; Sivaraj et al., 2001; Tsai et al., 2001; Annadurai et al., 2002; Namasivayam and Kavitha, 2002; Robinson et al., 2002) have also been reported. However, the adsorption capacities of the above adsorbents are not very high; some even less than 50 mg $g^{-1}$. In order to improve the efficiency of the adsorption processes, it is necessary to develop cheap and easily available adsorbents with high adsorption capacities.

Chitosan has been reported with the high potential for the adsorption of anionic dyes (Wu et al., 2000). The literature showed that the adsorption capacities of reactive dyes in neutral medium on chitosan were approximately 1000–1100 mg $g^{-1}$. Chitosan is the deacetylated form of chitin, which is a linear polymer of acetylamino-D-glucose and the nature abundance is next to cellulose. According to our previous study (Chiou and Li, 2003), the high contents of amino functional groups in chitosan might form the electrostatic attraction between the chitosan and anionic dyes.

The aim of this research is to investigate the adsorption behavior of chitosan in an acid medium. This is because the amino groups of chitosan are much more easily to be protonated at a pH below 6 and can form electrostatic attraction to adsorb a quantity of dye anions (Yoshida et al., 1993). Unfortunately, chitosan in acid solutions is also easily dissolved due to its protonated primary amino groups. Hence the use of chitosan as an adsorbent in removing dyes could be severely restricted due to its dissolving tendency in the acid effluent.

Some cross-linking reagents (Zeng and Ruckenstein, 1996) have been used to stabilize chitosan in acid solutions. Cross-linked chitosan is not only insoluble in an acid solution but is also endowed with stronger mechanical properties. Yoshida et al. (1993) used Denacol EX841 as a cross-linking reagent and obtained a high adsorption capacity (1200–1700 mg $g^{-1}$) of Orange II on the cross-linked chitosan fibers in acid solutions of pH 3.0 and 4.0. In our previous work (Chiou and Li, 2003), chitosan was cross-linked by epichlorohydrin (ECH) and exhibited a high adsorption capacity (1802–1840 mg $g^{-1}$) of reactive dye (RR189) on the cross-linked chitosan beads in acid aqueous solutions at 30 °C, pH 3.0. It appears technically feasible to remove acid and reactive dyes from acid aqueous solutions by cross-linked chitosan.

In this research, we investigated the equilibrium and kinetics of adsorption of two anionic dyes in acid solutions. The Langmuir equation was used to fit the equilibrium isotherm. The effects of solution pH on adsorption capacity were also studied. The dynamical behaviors of the adsorption were measured on the effect of initial dye concentration. The adsorption rates were determined quantitatively and stimulated by the nonlinear first-order and second-order models. The dynamical behavior of the removal of ADMI (American Dye Manufacturer Institute) (Allen et al., 1973) and of the dyes in mixture solutions was investigated. The competitive adsorption behavior of the two dyes in mixture solutions was also analyzed in the cases of lower and higher initial dye concentrations.

## 2. Materials and methods

### 2.1. Chemicals

Chitosan (α-type; extracted from snow crab shell, degree of deacetylation: 95.5%; average M/M: 200 kD) was supplied by OHKA Enterprises Co. and used as received. Reagents: ECH (⩾98%) and sodium tripolyphosphate (TPP) (⩾98%) were purchased from Fluka. The anionic dyes studied were supplied by Sigma–Aldrich Co. and used with no pretreatment. The purity of the dyes MY and RB15 are approximately 70% and 35%, respectively. These purities were used to convert all data into the true values. The structures of anionic dye MY and RB15 are displayed in Fig. 1.

### 2.2. Preparation of chitosan beads

The preparation of cross-linked chitosan beads is described by following our previous research (Chiou and Li, 2003). Chitosan powder (10.0 g) was dissolved in 1.0 $dm^3$, 1.5 wt.% of acetic acid solution and vigorously

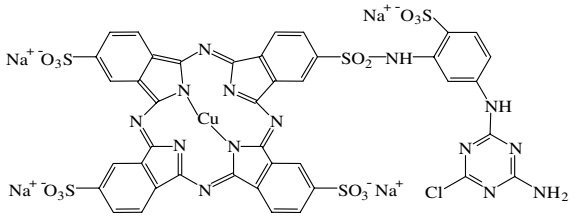

(a) RB15

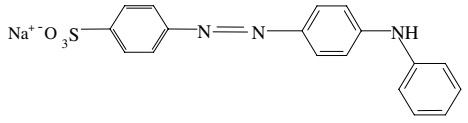

(b) Metanil Yellow

Fig. 1. The structure of anionic dyes.

stirred overnight, and then left still for 6 h. The chitosan solution (10 $cm^3$) was dropped from the burette into a 100 $cm^3$ aqueous solution of TPP (1 wt.%) and formed more rigid beads of diameters 2.3–2.5 mm. The ionic cross-linked chitosan beads were washed with deionized water, and stored them in distilled water. In order to stabilize chitosan in acid solution, the above ionically cross-linked chitosan beads, 50 $cm^3$ of 1 N sodium hydroxide solution, and chemical cross-linking reagent ECH were mixed and shaken for 6 h at 50 °C with a water bath (Deng Yng corp., Taiwan). The molar ratio of cross-linking reagent/chitosan was 0.5 in this work.

### 2.3. Batch equilibrium studies

Anionic dye solutions were prepared by dissolving dye in deionized water to the required concentrations. A buffer solution (10 $cm^3$, 0.1 M acetic acid/acetate) was added into a 40 $cm^3$ dye solution to maintain a fixed pH value. In the experiments of equilibrium adsorption isotherm, the mixture of chitosan beads (containing 0.1 g dry basis of chitosan) and 50 $cm^3$ dye solution (containing the buffer solution at pH 4) were shaken for 5 d using a water bath to control the temperature at 30 ± 1 °C. The pH of solutions will slightly increase during the adsorption processes and concentrated HCl was added to maintain the pH at a constant value. In order to measure the residual concentrations at same pH, the solutions were adjusted to pH 6.0 and analyzed with an UV/visible spectrometer (JASCO V-530) at wavelength corresponding to the maximum absorbance ($\lambda_{max}$). Since the $\lambda_{max}$ of dye solution might shift to different wavelength particularly at different pH (Bousher et al., 1997), the pH of diluted residual solutions was fixed at pH 6 before measuring the absorbance. In this work, the $\lambda_{max}$ for MY and RB15 are 434 nm and 674 nm at pH 6.0, respectively.

### 2.4. Batch kinetic studies

In the experiments of batch kinetic adsorption, a mixture of the cross-linked chitosan beads (0.1 g dry basis of chitosan) and 50 $cm^3$ of dye solution were shaken using a shaker with a water bath to control temperature. Similarly, concentrated HCl was used to maintain the dye solution at pH of 4. At regular intervals, 0.1 $cm^3$ of dye solution was taken out to dilute to 10 $cm^3$. Its concentration was also determined using UV/visible spectrometer after the pH was adjusted to 6.

The adsorption kinetics of a mixture of the two dyes onto the cross-linked chitosan beads at pH 4 was studied using the ADMI method (APHA, 1998). This method is applicable to colored waters and wastewaters having color characteristic. In our experiment, a mixture of the cross-linked chitosan beads (0.1 g dry basis of chitosan) and 50 $cm^3$ dye-mixture solution were shaken in a shaker at 30 °C. Concentrated HCl was used to maintain the dye solution at pH of 4. At regular intervals, 0.1 $cm^3$ of dye-mixture solution was taken out to dilute to a proper ADMI range (0–250 color unit (c.u.)). The ADMI color values were determined using a spectrophotometer (HACH DR/4000) with a narrow (10 nm or less) spectral band and an effective operating range of 400–700 nm after the pH of diluted residual solution was adjusted to 7.6.

## 3. Results and discussion

### 3.1. Effect of pH

Fig. 2 shows the effect of pH on equilibrium adsorption of the anionic dyes onto the cross-linked chitosan beads at 30 °C. The pH significantly affected the adsorption capacities of the anionic dyes onto the cross-linked chitosan beads. In general, the uptakes were much higher in acidic solutions than those in neutral and alkaline conditions. The maximum values of the adsorption capacity ratio between acidic and alkaline conditions reached 9.3, and 5.0 for MY (pH 4/8) and RB15 (pH 3/8), respectively.

According to Yoshida et al. (1993), at lower pH more protons will be available to protonate amino groups of chitosan molecules to form $-NH_3^+$ groups, thereby increasing the electrostatic attractions between negatively charged dye anions and positively charged adsorption sites and causing an increase in dye adsorption. This explanation agrees with our data on pH effect. It can be seen that the pH of aqueous solution plays an important role in the adsorption of anionic dyes onto chitosan.

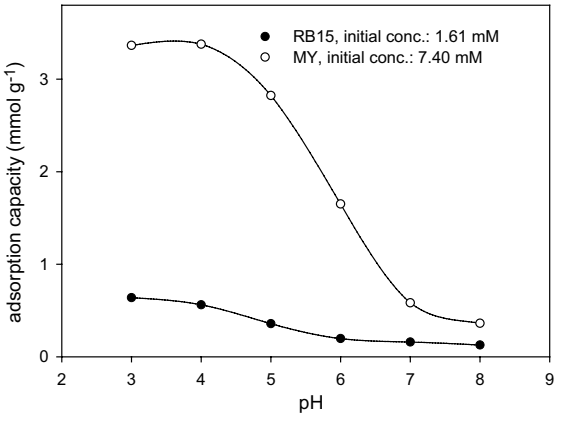


Fig. 2. The effect of pH on the adsorption capacity of dyes RB15 and MY onto cross-linked chitosan beads at 30 °C.

### 3.2. Adsorption isotherms

Fig. 3 shows the adsorption isotherms of the two dyes at pH 4, 30 °C using the cross-linked chitosan beads. The equilibrium adsorption density $q_e$ increased with the increase in dye concentration. The shape of the isotherm of RB15 looks rectangular because at low equilibrium dye concentrations $C_e$, the equilibrium adsorption densities $q_e$ of the cross-linked chitosan beads reach almost the same $q_e$ as those at high equilibrium dye concentrations. It indicates that the cross-linked chitosan beads have high adsorption density even at low equilibrium dye concentrations. Comparing the two isotherms in Fig. 3, the $q_e$ of MY is much greater than that of RB15 as $C_e$ is greater than 0.05 mM. It is because that the molecular size of MY is much smaller than that of RB15 (Fig. 1), and more molecules of a smaller dye can be uptaken by per unit weight of the adsorbent.

Parameters of the Langmuir isotherms were computed in Table 1. The Langmuir isotherm fits quite well with the experimental data (correlation coefficient $R^2 > 0.996$). Table 1 indicates that the computed maximum monolayer capacity $Q$ on the cross-linked chitosan beads has a large value of 3.56 mmol $g^{-1}$ (1334 mg $g^{-1}$) for dye MY and 0.56 mmol $g^{-1}$ (722 mg $g^{-1}$) for dye RB15. By accounting the degree of deacetylation (95.5%) and the molecular weight of repeating unit of the chitosan (161.16 g $mol^{-1}$), the mole of the adsorption site $-NH_3^+$ is 5.93 mmol $g^{-1}$. Without considering the portion of $-NH_3^+$ used in cross-linking, the coverage of dyes MY and RB15 onto the cross-linked chitosan is roughly estimated to be 60% and 10%, respectively. The great difference in coverage is caused by the molecule size of RB15, which is much larger than that of MY. It is difficult for the large RB15 molecule to diffuse into some small pores in the chitosan, and one adsorbed molecule of RB15 blocks more adsorption sites $-NH_3^+$ on the chitosan beads to uptake another dye molecules.

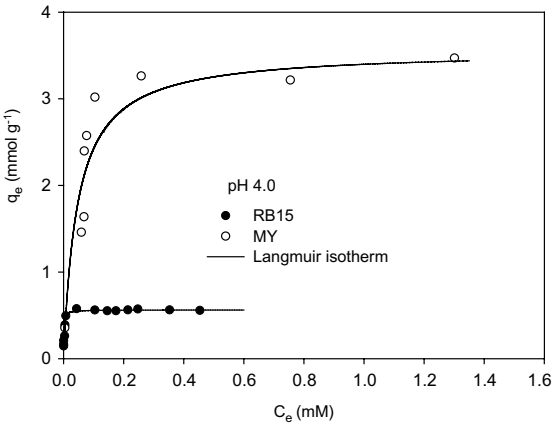


Fig. 3. Equilibrium adsorption isotherm of dyes on cross-linked chitosan beads.

Table 1
Langmuir isotherm constants for anionic dye at pH 4, 30 °C

| Dye | Langmuir equation | | |
|---|---|---|---|
| | $Q$ (mmol $g^{-1}$) | $b$ ($dm^3$ $mmol^{-1}$) | $R^2$ |
| MY | 3.56 | 21.35 | 0.996 |
| RB15 | 0.56 | 895.12 | 1.000 |

### 3.3. Effect of initial dye concentration

Figs. 4 and 5 show the effect of initial dye concentration on the adsorption kinetics of the cross-linked chitosan at 30 °C, pH 4 for RB15 and MY, respectively. An increase in initial dye concentration led to an increase in the adsorption capacity of dye on chitosan. According to Fig. 4a, the adsorption capacities of RB15 for 10 h with initial dye concentrations at 1.36, 1.12, 0.97 and 0.81 mM were 99%, 89%, 71% and 45% greater than that at 0.55 mM, respectively. Fig. 5a shows that the adsorption capacity of MY for 6 h with initial dye concentrations at 5.63 and 3.78 mM were 100% and 36% greater

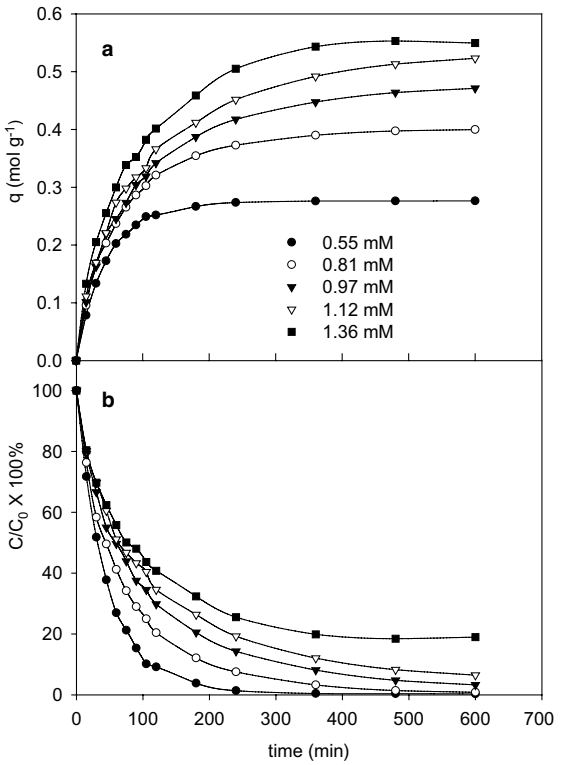


Fig. 4. The effect of initial dye concentration on the adsorption kinetics of RB15 on cross-linked chitosan beads at pH 4, 30 °C.

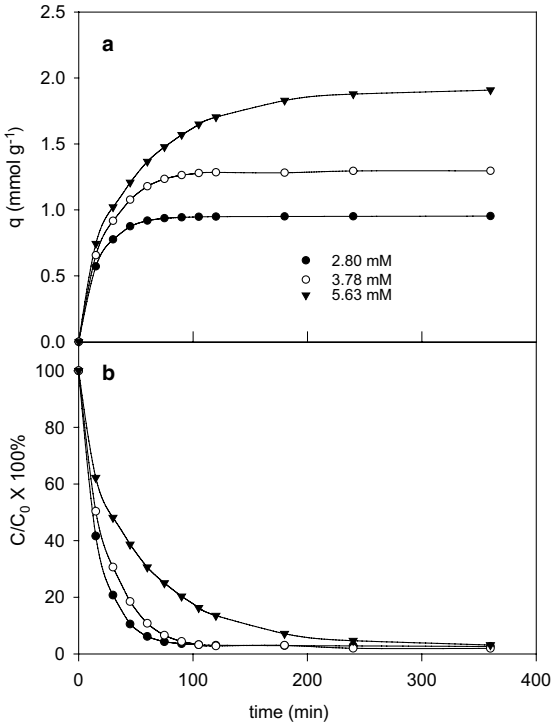


Fig. 5. The effect of initial dye concentration on the adsorption kinetics of MY on cross-linked chitosan beads at pH 4, 30 °C.

than that at 2.80 mM, respectively. These indicate that the initial dye concentrations played an important role in the adsorption capacities of MY and RB15 on the cross-linked chitosan beads.

Figs. 4b and 5b show the effect of initial dye concentration on the kinetics of the residual concentration ratio ($C/C_0$) in the solution at 30 °C, pH 4 for RB15 and MY, respectively. Both Figs. 4b and 5b imply that the decreasing rate of the residual concentration ratio increases with decreasing initial dye concentrations. Fig. 4b indicates that the residual concentration ratio of RB15 almost approaches zero after 10 h for initial concentration at 0.55 and 0.81 mM, while the adsorption reaches saturation for initial concentration at 1.36 mM due to its high residual concentration ($C_e$ = 0.26 mM). Fig. 5b indicates that the residual concentration ratio of MY remains a very low concentration after 6 h for the three initial concentrations under study.

In order to investigate the mechanism of adsorption, the first-order and second-order adsorption models were used to test dynamical experimental data by nonlinear regression. Table 2 lists the results of rate constant studies for different initial dye concentrations by the first-order and second-order models. Considering both the equilibrium adsorption $q_e$ and the correlation coefficient $R^2$ in Table 2, for both dyes MY and RB15 the first-order kinetic model fits better in lower initial dye concentrations; while the second-order kinetic model fits better in higher initial dye concentrations. This is because the adsorption driving force for higher initial dye concentrations is stronger than that for lower initial concentrations. Thus, the faster second-order model describes experimental data more adequately for higher initial concentrations.

### 3.4. Removal of ADMI in dye mixtures

The wastewater from industry usually contains more than one dye. To study the adsorption behavior of dye mixtures, the adsorption kinetics of mixtures of the two anionic dyes onto the cross-linked chitosan beads at pH 4, 30 °C were studied by the removal of ADMI from aqueous solutions. ADMI removal percent (%) is the ratio between the removal ADMI value at any contact time and the ADMI value at initial concentration. Two different mixtures were studied. The lower initial concentration (solution A) consists of MY: 1.57 (mM)

Table 2
Comparison of the nonlinear first-order[a] and second-order[b] adsorption rate constants, calculated $q_e$ and experimental $q_t$ values for different initial dye concentrations at pH 4, 30 °C

| Dye | Initial dye conc. (mM) | $q_t$ (mmol g$^{-1}$) | First-order kinetic model | | | Second-order kinetic model | | |
|---|---|---|---|---|---|---|---|---|
| | | | $k_1$ (min$^{-1}$) | $q_{e,cal}$ (mmol g$^{-1}$) | $R^2$ | $k_2$ (g mmol$^{-1}$ min$^{-1}$) | $q_{e,cal}$ (mmol g$^{-1}$) | $R^2$ |
| MY (6 h) | 2.80 | 0.95 | 5.91E-02 | 0.95 | 0.997 | 1.02E-01 | 1.02 | 0.929 |
| | 3.78 | 1.30 | 4.31E-02 | 1.29 | 0.993 | 4.74E-02 | 1.42 | 0.953 |
| | 5.63 | 1.91 | 2.46E-02 | 1.83 | 0.958 | 1.53E-02 | 2.11 | 0.993 |
| RB15 (10 h) | 0.55 | 0.28 | 2.19E-02 | 0.28 | 0.999 | 9.92E-02 | 0.31 | 0.969 |
| | 0.81 | 0.40 | 1.57E-02 | 0.39 | 0.987 | 4.50E-02 | 0.44 | 0.997 |
| | 0.97 | 0.47 | 1.27E-02 | 0.45 | 0.983 | 2.84E-02 | 0.53 | 0.999 |
| | 1.12 | 0.52 | 1.17E-02 | 0.50 | 0.978 | 2.30E-02 | 0.59 | 0.998 |
| | 1.36 | 0.55 | 1.29E-02 | 0.54 | 0.976 | 2.51E-02 | 0.62 | 0.995 |

[a] Nonlinear first-order model: $q_t = q_e(1 - e^{-k_1 t})$.
[b] Nonlinear second-order model: $q_t = \frac{q_e^2 k_2 t}{1+q_e k_2 t}$.

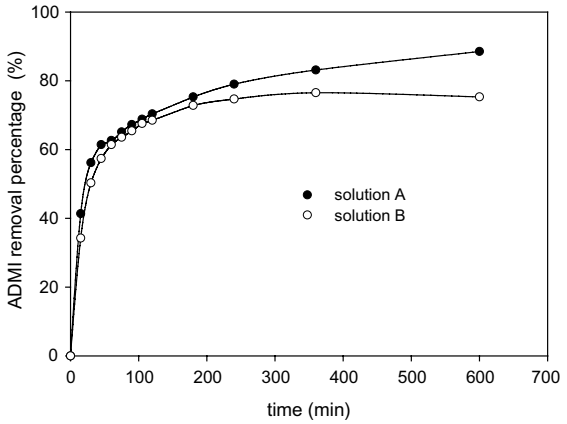


Fig. 6. The kinetics of ADMI removal of a dye mixture solution for different initial concentrations (ADMI for solution A: 162000 c.u.; solution B: 324000 c.u.) at pH 4 and 30 °C.

and RB15: 0.73, whose ADMI is equal to 162000 c.u. The higher initial concentration (solution B) consists of MY: 3.00 (mM) and RB15: 1.34, whose ADMI is equal to 324000 c.u., respectively. Fig. 6 indicates that the ADMI removal of the mixture of the dye solution increased with contact time for two different initial concentrations. The equilibrium removal percentages of ADMI for lower initial concentrations (solution A) are larger than those for higher initial concentrations (solution B). Obviously, the sorbent in solution B was completely saturated due to the high equilibrium residual concentration ($C_e = 0.26$ mM) at initial concentration 1.36 mM of RB15 in Fig. 4b.

Similar to the adsorption kinetics of a single dye discussed above, the kinetics of the ADMI removal and of the dye mixture shown in Fig. 6 can be described by the nonlinear first-order and second-order rate model. Table 3 lists the results of ADMI rate constant studies by the nonlinear first-order and second-order models at pH 4 for two different initial concentrations. In Table 3, $D_e$ and $D_t$ are the removal percent (%) at equilibrium and at time $t$, respectively; $k_{d1}$ and $k_{d2}$ are the corresponding rate constants of the nonlinear first-order and second-order adsorption ($min^{-1}$), respectively. The correlation coefficient $R^2$ for the second-order adsorption model has a high value (>0.981), and its calculated equilibrium removal percent $D_{e2,cal}$ is consistent with the experimental data $D_t$ ($t = 10$ h). In Table 3, the experimental removal percent $D_t$ and calculated equilibrium removal percent $D_{e2,cal}$ of solution A are greater than those of solution B, since the adsorbent in solution B was saturated.

### 3.5. Competitive adsorption

The ADMI method discussed above allows us to understand the overall adsorption behavior of mixtures containing the two anionic dyes. Suppose there is no interaction between the two dyes, the total absorbance for a mixture dye solution is equal to the summation of the absorbance of each dye (Skoog et al., 1998). This is represented in Eq. (1a). To determine and analyze whether the existence of one dye affected the adsorption of another dye, the adsorption capacities of each dye in mixture solutions are computed using Eqs. (1b) and (1c).

$$A_\lambda = A_{MY} + A_{RB15} \quad (1a)$$

$$A_{\lambda 1} = \varepsilon_{1M} z C_{MY} + \varepsilon_{1R} z C_{RB15} \quad (1b)$$

$$A_{\lambda 2} = \varepsilon_{2M} z C_{MY} + \varepsilon_{2R} z C_{RB15} \quad (1c)$$

In Eqs. (1), $A_\lambda$, $A_{\lambda 1}$ and $A_{\lambda 2}$ are the absorbance of UV/visible spectrometer at wavelength $\lambda$, $\lambda_1$ and $\lambda_2$, respectively; $A_{MY}$ and $A_{RB15}$ are the absorbance of MY and RB15 at wavelength $\lambda$, respectively; $\varepsilon_{1M}$ and $\varepsilon_{2M}$ are the absorbance coefficient of pure MY at wavelength $\lambda_1$ and $\lambda_2$, respectively; $\varepsilon_{1R}$ and $\varepsilon_{2R}$ are the absorbance coefficient of pure RB15 at wavelength $\lambda_1$ and $\lambda_2$, respectively; $C_{MY}$ and $C_{RB15}$ are the concentration of MY and RB15 in the mixture solutions; $z$ is the cell width (1 cm); $\lambda_1$ (434 nm) is the wavelength of maximum absorbance for MY; and $\lambda_2$ (674 nm) is the wavelength of maximum absorbance for RB15. The concentrations $C_{MY}$ and $C_{RB15}$ are solved from Eqs. (1b) and (1c) and then calculated to obtain the adsorption capacity for each dye in mixture solutions.

Fig. 7a shows the kinetics of the competitive adsorption in mixture solution C at pH 4 and 30 °C, where dyes MY and RB15 have similar initial concentrations. In

Table 3
Comparison of the nonlinear first-order[a] ($k_{d1}$) and second-order[b] ($k_{d2}$) ADMI removal rate constants, calculated and experimental $d_t$ values of two different initial concentrations ($t = 10$ h, pH = 4, 30 °C)

| Initial conc. (ADMI) | $D_t$ (%) | First-order kinetic model | | | Second-order kinetic model | | |
|---|---|---|---|---|---|---|---|
| | | $k_{d1}$ ($min^{-1}$) | $D_{e2,cal}$ (%) | $R^2$ | $k_{d2}$ ($min^{-1}$) | $D_{e,cal}$ (%) | $R^2$ |
| A: 1.62E5 | 89 | 3.87E-2 | 76 | 0.922 | 6.48E-4 | 85 | 0.981 |
| B: 3.24E5 | 75 | 3.62E-2 | 72 | 0.979 | 6.86E-4 | 80 | 0.998 |

[a] $D_t = D(1 - e^{-k_{d1}t})$.

[b] $D_t = \frac{D_e^2 k_{d2} t}{1 + D_e k_{d2} t}$.

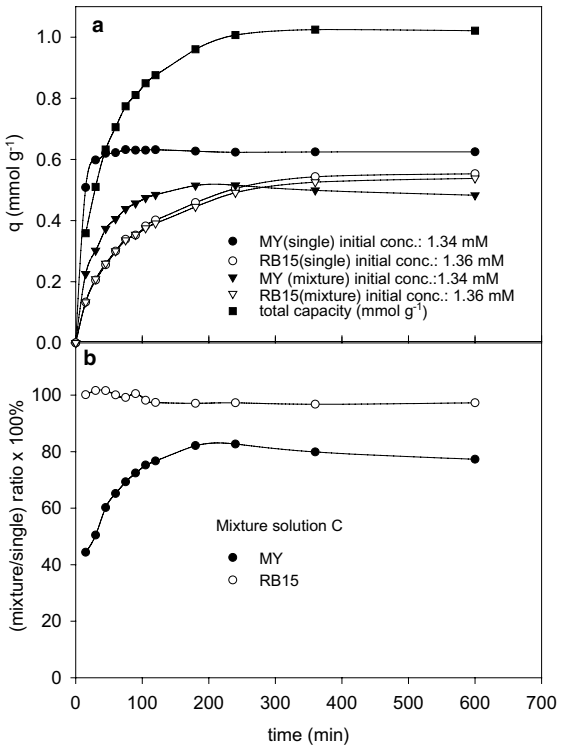


Fig. 7. (a) The kinetics of the adsorption capacity of the single and mixture dye solutions onto cross-linked chitosan beads at pH 4, 30 °C. (b) The ratio of the adsorption capacity between the mixture solution C and the single dye solution.

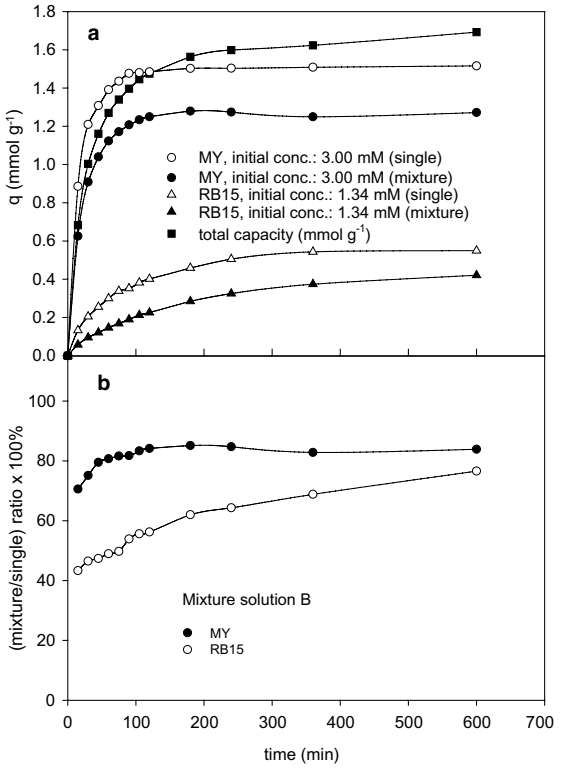


Fig. 8. (a) The kinetics of the adsorption capacity of single and mixture dye solutions with higher initial dye concentrations onto cross-linked chitosan beads at pH 4, 30 °C. (b) The ratio of the adsorption capacity between the mixture solution B and the single dye solution.

Fig. 7a, the adsorption capacity of each dye in a mixture was computed using the method mentioned above and the curve, total capacity, represented the sum of the adsorption capacity of the two dyes in a mixture. Fig. 7a also shows that the initial adsorption rate of MY onto the chitosan beads is faster than that of the RB15; and the time for MY to reach the adsorption equilibrium is shorter than that of RB15. This might be caused by the large difference between the molecule sizes of the two anionic dyes (see Fig. 1). The dye MY is much smaller than dye RB15 and it is easier for the molecule of MY to diffuse into the chitosan beads.

The adsorption kinetics of each single dye with the same initial concentrations as those in mixture solution C was also measured for comparisons. To understand which dye is affected more in the competitive adsorption, the data in Fig. 7a was transferred into the ratio (mixture/single) of the adsorption capacity shown in Fig. 7b. The ratio of RB15 remains almost 100% within a 10 h of contact time, while the ratio of MY increases with the contact time, starting from 44% and approaching 80% at about 200 min. It indicates that, in the mixture solution C, dye MY is affected apparently by the existence of the dye RB15 during the competitive adsorption while dye RB15 is almost unaffected by the dye MY at all.

To study the competitive adsorption in a mixture with a higher concentration of MY, the mixture solution B, consists of MY: 3.00 mM and RB15: 1.34 mM initially, is tested. Fig. 8 shows the kinetics of the competitive adsorption in mixture solution B at pH 4 and 30 °C. The adsorption rate of MY onto the chitosan beads is much faster than that of the RB15. The dye MY reaches the adsorption equilibrium at about 2 h, while RB15 still does not approach equilibrium even at 10 h. The adsorption kinetics of each single dye with the same initial concentrations as those in mixture solution B was also measured for comparisons. To understand which dye is more favorable in the competitive adsorption, the data in Fig. 8a was transferred into the ratio (mixture/single) of the adsorption capacity shown in Fig. 8b. The ratio of MY reaches 80% at 2 h, that is larger than that of RB15 within a 10 h of contact time. The ratio of RB15 increases with contact time, starting from 42% and approaching 75% at 10 h. It indicates that the adsorption kinetics of the two dyes affects each

Table 4
Comparison of the nonlinear first-order and second-order adsorption rate constants, calculated $q_e$, experimental $q_t$ values and intraparticle diffusion parameters for different initial dye concentrations at 30 °C, pH 4, $t = 10$ h

| Mixture | Initial conc. (mM) | $q_t$ (mmol g$^{-1}$) | First-order kinetic model | | | Second-order kinetic model | | | Intraparticle diffusion model | |
|---|---|---|---|---|---|---|---|---|---|---|
| | | | $k_1$ (min$^{-1}$) | $q_{e,cal}$ (mmol g$^{-1}$) | $R^2$ | $k_2$ (g mmol$^{-1}$ min$^{-1}$) | $q_{e,cal}$ (mmol g$^{-1}$) | $R^2$ | $k_{p,2}$ (mmol g$^{-1}$ min$^{-0.5}$) | $k_{p,3}$ (mmol g$^{-1}$ min$^{-0.5}$) |
| *Solution C* | | | | | | | | | | |
| MY | 1.34 | 0.48 | 3.16E-2 | 0.50 | 0.989 | 2.07E-1 | 0.54 | 0.983 | 4.51E-2 | 1.58E-2 |
| RB15 | 1.36 | 0.54 | 1.40E-2 | 0.51 | 0.981 | 2.93E-2 | 0.60 | 0.998 | 4.22E-2 | 2.27E-3 |
| *Solution B* | | | | | | | | | | |
| MY | 3.00 | 1.27 | 4.19E-2 | 1.25 | 0.997 | 5.05E-2 | 1.36 | 0.989 | 9.49E-2 | 3.97E-2 |
| RB15 | 1.34 | 0.42 | 6.86E-3 | 0.42 | 0.993 | 1.20E-2 | 0.52 | 0.998 | 2.35E-2 | 1.05E-2 |

other, and the competitive adsorption favors the dye MY in the mixture solution B. Beside the reason of the smaller molecule size of MY, another major factor is that dye MY contains higher initial molar concentration and exhibits a stronger driving force for the adsorption process.

Table 4 shows the analysis of the adsorption rate constant and equilibrium adsorption capacity by the nonlinear first-order and second-order kinetic models for both mixture solutions B and C. By judging the $q_{e,cal}$ and $R^2$ in Table 4, the first-order model fits well and better than the second-order model for dye MY in both solutions B and C. This result is similar to that for dye MY in the Table 2 as it is in a lower initial dye concentrations. For dye RB15 in Table 4, the second-order model fits well and better than the first-order model in solution C. However, the first-order model fits well and better than the second-order model for dye RB15 in solution B, for which dye RB15 has a similar initial dye concentration as that in solution C. This shows an interesting phenomenon that the adsorption kinetic model has the tendency to shift from the second order to the first order for dye RB15 as the concentration of the competitor dye MY changes from a lower value (solution C) to a higher value (solution B). It indicates that in the mixture solution B the adsorption rate of RB15 onto the chitosan beads is slowed down by the adsorption of the dye MY. Thus, its adsorption kinetic model shifts from the fast model (the second order) to the slow model (the first order) in the competitive adsorption processes. The contribution of resistance to internal diffusion might be the reason (see the discussions in the next section).

### 3.6. Intraparticle diffusion model

The intraparticle diffusion model (Weber and Morris, 1962) was applied to describe the competitive adsorption for mixture solutions B and C. In a liquid-solid system, the fractional uptake of the solute on particle varies according to a function of $[(D_t)^{0.5}/r]$, where $D$ is the diffusivity within the particle and $r$ is the particle radius. The initial rates of intraparticle diffusion are obtained by linearization of the curve $q_t = f(t^{0.5})$. The plot of $q_t$ against $t^{0.5}$ may present a multi-linearity (Allen et al., 1989), which indicates that two or more steps occur in the adsorption processes. The first sharper portion is external surface adsorption or instantaneous adsorption stage. The second portion is the gradual adsorption stage, where the intraparticle diffusion is rate-controlled. The third portion is the final equilibrium stage, where the intraparticle diffusion starts to slow down due to the extremely low solute concentration in solution.

Fig. 9 shows the plot of $q_t$ against $t^{0.5}$ for the competitive adsorption occurring in mixture solutions B and C. The slope of the line in each stage is written as the rate

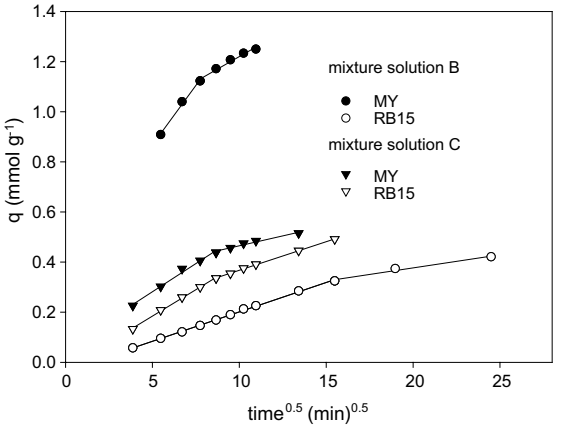


Fig. 9. The intraparticle diffusion model to describe the competitive adsorption for mixture solutions B and C.

parameter $k_{p,i}$ ($i$ = 1–3). Since the first stage (external surface adsorption) is completed fast and is less apparent, Fig. 9 only shows the second stage (intraparticle diffusion) and the third stage (equilibrium). The corresponding rate parameters are listed in Table 4. Table 4 indicates that the order of adsorption rate is $k_{p,2} > k_{p,3}$ for each dye in mixtures. In mixture solutions C with similar initial dye concentrations, the $k_{p,2}$ of MY is slightly greater than the $k_{p,2}$ of RB15. It is because the molecule of MY is smaller and it diffuses faster. However, the $k_{p,3}$ of MY becomes smaller than that of RB15 in solution C. It indicates that the existence of dye RB15 does affect the diffusion rate of dye MY inside the chitosan beads. In the solution B, where the initial concentration of MY is more than twice of that of RB15, the $k_{p,2}$ and $k_{p,3}$ of MY are much greater than those of RB15. It is not only caused by the effect of molecule size but also by the effect of initial concentration. The competitive adsorption apparently favors the dye MY in the solution B.

## 4. Conclusions

This study investigated the equilibrium and the dynamics of the adsorption of two anionic dyes on the chemically cross-linked chitosan beads. The cross-linked chitosan beads had high adsorption capacities to remove the anionic dyes, whose maximum monolayer adsorption capacity is 3.56 mmol $g^{-1}$ (1334 mg $g^{-1}$) for dye MY and 0.56 mmol $g^{-1}$ (722 mg $g^{-1}$) for dye RB15 at pH 4, 30 °C. The adsorption capacities were significantly affected by the initial dye concentration and pH. The uptake increased with increase in initial dye concentration and with decrease in pH. The strong electrostatic interaction between the $-NH_3^+$ of chitosan and dye anions can be used to explain the high adsorption capacity of anionic dyes onto chemically cross-linked chitosan beads. The equilibrium isotherm agrees very well with the Langmuir equation. The first-order kinetic model fits well with the dynamical adsorption behavior of a single dye for lower concentrations, while the second-order kinetic model fits well for higher dye concentrations. In mixture solution C (initial conc. (mM): MY = 1.34; RB15 = 1.36), the adsorption of the dye MY is affected significantly by the existence of dye RB15, while the adsorption of dye RB15 is almost unaffected by the dye MY. In the mixture solutions B (initial conc. (mM): MY = 3.00; RB15 = 1.34), the adsorption kinetics of the two dyes affect each other, the competitive adsorption favors the dye MY, and the adsorption kinetic model of RB15 has the tendency to shift to the slower first-order model.

## References

Allen, S.J., 1996. Types of adsorbent materials. In: McKay, G. (Ed.), Use of Adsorbents for the Removal of Pollutants from Wastewaters. CRC, Inc., Boca Raton, FL, USA, pp. 59–97.

Allen, S.J., McKay, G., Khader, K.Y.H., 1989. Intraparticle diffusion of a basic dye during adsorption onto sphagnum peat. Environ. Pollut. 56, 39–50.

Allen, W., Prescott, W.B., Derby, R.E., Garland, C.E., Peret, J.M., Saltzman, M., 1973. Determination of color of water and wastewater by means of ADMI color values. In: Proceedings of the 28th Purdue Industrial Waste Conference. Purdue University, West Lafayette, IN, pp. 661–675.

Annadurai, G., Juang, R.S., Lee, D.J., 2002. Use of cellulose-based wastes for adsorption of dyes from aqueous solutions. J. Hazard. Mater. 92, 263–274.

APHA, American Public Health Association, 1998. Standard Method for the Examination of Water and Wastewater, 20th ed., method 2120 E. APHA–AWWA–WEF, Washington, DC, USA.

Bousher, A., Shen, X., Edyvean, R.C.J., 1997. Removal of coloured organic matter by adsorption onto low-cost waste materials. Water Res. 31, 2084–2092.

Chiou, M.S., Li, H.Y., 2003. Adsorption behavior of reactive dye in aqueous solution on chemical cross-linked chitosan beads. Chemosphere 50, 1095–1105.

Choudhary, G., 1996. Human health perspective on environmental exposure to benzidine: a view. Chemosphere 32, 267–291.

Low, K.S., Lee, C.K., 1997. Quaternized rice husk as sorbent for reactive dyes. Bioresour. Technol. 61, 121–125.

McKay, G., 1984. Analytical solution using a pore diffusion model for a pseudo-irreversible isotherm for the adsorption of basic dye on silica. AIChE J. 30, 692–697.

McKay, G., Blair, H.S., Gardner, J.R., 1983. Rate studies for the adsorption of dyestuffs on chitin. J. Colloid Interf. Sci. 95, 108–119.

Namasivayam, C., Kavitha, D., 2002. Removal of Congo Red from water by adsorption onto activated carbon prepared from coir pith, an agricultural solid waste. Dyes Pigments 54, 47–58.

Rao, K.C.L.N., Ashutosh, K.K., 1994. Color removal from dyestuff industry effluent using activated carbon. Indian J. Chem. Tech. 1, 13–19.

Ramakrishna, K.R., Viraraghavan, T., 1997. Dye removal using low cost adsorbents. Water Sci. Technol. 36, 189–196.

Robinson, T., Chandran, B., Nigam, P., 2002. Removal of dyes from a synthetic textile dye effluent by biosorption on apple pomace and wheat straw. Water Res. 36, 2824–2830.

Sivaraj, R., Namasivayam, C., Kadirvelu, K., 2001. Orange peel as an adsorbent in the removal of acid violet 17 (acid dye) from aqueous solutions. Waste Manage. 21, 105–110.

Skoog, D.A., Holler, F.J., Nieman, T.A., 1998. Principles of Instrumental Analysis, fifth ed. Saunders College Publishing, Philadelphia, USA, p. 303.

Tsai, W.T., Chang, C.Y., Lin, M.C., Chien, S.F., Sun, H.F., Hsieh, M.F., 2001. Adsorption of acid dye onto activated carbon prepared from agricultural waste bagasse by $ZnCl_2$ activation. Chemosphere 45, 51–58.

Weber, W.J., Morris, J.C., 1962. Advances in water pollution research: removal of bio-logically resistant pollutants from waste waters by adsorption. International Conference On Water Pollution Symposium, vol. 2. Pergamon, Oxford, pp. 231–266.

Wu, F.C., Tseng, R.L., Juang, R.S., 2000. Comparative adsorption of metal and dye on flake- and bead-types of chitosans prepared from fishery wastes. J. Hazard. Mater. B73, 63–75.

Yoshida, H., Okamoto, A., Kataoka, T., 1993. Adsorption of acid dye on cross-linked chitosan fibers: equilibria. Chem. Eng. Sci. 48, 2267–2272.

Yu, M.C., Skipper, P.L., Tannenbaum, S.R., Chan, K.K., Ross, R.K., 2002. Arylamine exposures and bladder cancer risk. Mutat. Res.-Fund. Mol. M. 506–507, 21–28.

Zeng, X.F., Ruckenstein, E., 1996. Control of pore sizes in macroporous chitosan and chitin membranes. Ind. Eng. Chem. Res. 35, 4169–4175.